International Journal of Electrical, Electronic and Communication Sciences
ISSN: 2517-9438
Vol:2, No:3, 2008

Central Pattern Generator Incorporating the Actuator Dynamics for a Hexapod Robot

Valeri A. Makarov, Ezequiel Del Rio, Manuel G. Bedia, Manuel G. Velarde, and Werner Ebeling

***Abstract*—** We proposed the use of a Toda-Rayleigh ring as a central pattern generator (CPG) for controlling hexapodal robots. We show that the ring composed of six Toda-Rayleigh units coupled to the limb actuators reproduces the most common hexapodal gaits. We provide an electrical circuit implementation of the CPG and test our theoretical results obtaining fixed gaits. Then we propose a method of incorporation of the actuator (motor) dynamics in the CPG. With this approach we close the loop CPG – environment – CPG, thus obtaining a decentralized model for the leg control that does not require higher level intervention to the CPG during locomotion in a nonhomogeneous environments. The gaits generated by the novel CPG are not fixed, but adapt to the current robot bahvior.

***Keywords*—** Central pattern generator, electrical circuit, hexapod robot

I. Introduction

Animal locomotion is driven by a central pattern generator (CPG), which is an intra-spinal network of neurons capable of generating a rhythmic output required for the limb control [1]. The study of CPGs is crucial for understanding both the global animal behaviour and particular functions of such neural networks. Besides it is also important for designing of neuro-inspired robots capable to move in an efficient manner like the living organisms do.

Recently, research on the leg coordination and movement has been shifted from descriptive studies [2] to investigations of the neurophysiological mechanisms and control of walking [3]. The architecture of CPGs is seldom observable in vivo [4]. However, important aspects of their structure can be inferred from observation of gait features such as the phase of the gait cycle at which a given limb hits the ground. Then phenomenological models reproducing these features can be introduced and used for the robot design. Inspired by this idea the use of oscillatory neural network with different architectures has been argued [5], [6] to solve the problem of dynamical pattern formation and robust transition among several types of gaits.

In fact, most animal gaits possess a degree of symmetry and universal features not far from the behavior of rings of coupled oscillators [7]. It has been shown that coupled nonlinear oscillators can be considered as possible models for locomotor CPGs in insects and other animals [4], [8]-[11]. Then transitions between different gaits can be modeled as a symmetry breaking bifurcation, leading to the switch between different activity patterns in a ring.

In this paper we approach the problem of locomotion control from the nonlinear dynamics viewpoint. We make remarkable parallels between waves observed in coupled nonlinear oscillators and the symmetries found in animal gaits. We describe how this observation might impose constraints on the general structure of a neural circuit controlling locomotion. To demonstrate the approach we consider a ring of coupled oscillators whose nonlinear elements are drawn from works of Lord Rayleigh and Toda [12]-[14]. In our earlier works [15], [16] we proposed a method of combination of hamiltonian Toda inter-particle nonlinearity with the Rayleigh active friction. We showed theoretically and numerically existence and stability of propagating wave in such a hybrid system. Further several hardware implementations of the six-units model have been developed and tested [17]. Here we extend our results and show that the excitation patterns (waves) in a ring of coupled Toda-Rayleigh oscillators have the same symmetries and waveforms as the three common forward-walking gaits adopted by insects. In earlier works [4], [6]-[11], [18] gaits have been considered as fixed oscillatory rhythms. However, insects (and other animals e.g. crustaceans) apply free gaits, changing rhythms according to the environment. We propose a method how to incorporate the actuator (motor) dynamics in the CPG based on the Toda-Rayleigh circuit, hence closing the loop CPG – environment – CPG. Thus our approach naturally permits to perform extensive calculations during locomotion over a nonhomogeneous environment on the low CPG level with no direct participation of the robot "brain".

II. Most common hexapodal gaits

Animal locomotion typically employs several distinct periodic patterns of leg movements, known as gaits. Most of the gaits possess some degree of symmetry. Let us now briefly describe the symmetries observable in hexapodal gaits.

Figure 1 illustrates the most common gaits of an insect (for more details see e.g. [9]). We use the following convention: the limbs on the left and right sides are numbered starting from

This research has been supported in part by the European Union under SPARK grant (FP6-2003-IST-004690), by Universidad Complutense de Madrid under the grant PR1/06-14482-B and by the Spanish Ministerio de Educacion y Ciencia under the grant ESP2004-01511, and a Ramon y Cajal grant (awarded to VAM).

V. A. Makarov is with Escuela de Optica, Universidad Complutense, Avda. Arcos de Jalon s/n, Madrid 28037, Spain.

E. Del Rio is with E.T.S.I. Aeronauticos, Universidad Politecnica, Plaza Cardenal Cisneros, 3, Madrid 28040, Spain.

M. G. Bedia is with Escuela Politecnica Superior, Universidad Carlos III, Avda. de la Universidad, 30, Madrid 28911, Spain.

M. G. Velarde is with Instituto Pluridisciplinar, Universidad Complutense, Paseo Juan XXIII, 1, Madrid 28040, Spain.

W. Ebeling is with Institut für Physik, Humboldt Universität, Berlin D-12489, Germany.

the frontal leg and marked by letters L and R, respectively (Fig. 1A).

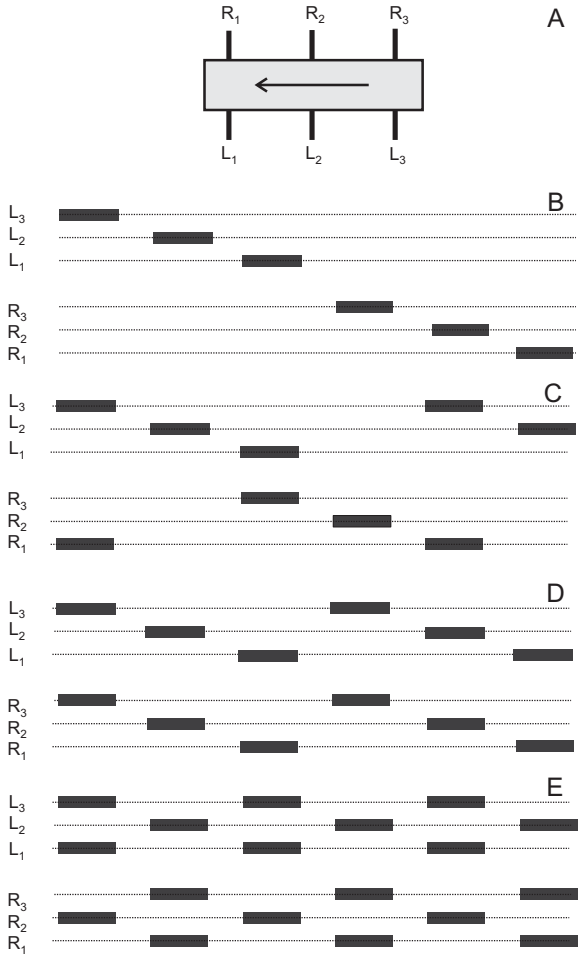

Fig. 1. Sketch of the most common hexapod gaits. A) Leg numbering convention. Letters L and R codify the left and right sides of the agent, respectively, while the subindex stands for the limb number. B) Metachronal (low – speed) gait. Thick segments show the swing phases (or the return stroke) dashed segments correspond the the stance phases (or the power stroke). No more than one leg at a time is lifted and moving forward. C) Ripple (medium – speed) gait. D) Canterpillar (medium – speed) gait. E) Tripod (fast – speed) gait.

When an insect moves slowly, it normally adopts the so called metachronal gait (Fig. 1B). This gait can be described as a "wave" propagating anteriorly from the back of the animal (first on the left side, and then on the rigth side) according to the scheme:

$$\mathrm{L_3},\ \mathrm{L_2},\ \mathrm{L_1},\ \mathrm{R_3},\ \mathrm{R_2},\ \mathrm{R_1}.$$

For this gait the adjacent limbs of each half of the insect body ($\mathrm{R_3}$ and $\mathrm{R_2}$, $\mathrm{R_2}$ and $\mathrm{R_1}$) are 60° out of phase. The limbs of each segment (e.g. $\mathrm{R_3}$ and $\mathrm{L_3}$) are half a period (or 180°) out of phase.

For moving with a medium speed, an insect usually adopts the ripple gait (Fig. 1C). Then the limb movement (swing phase) is described by:

$$(\mathrm{L_3R_1}),\ \mathrm{L_2},\ (\mathrm{L_1R_3}),\ \mathrm{R_2}.$$

Here brackets link the legs moving together. Accordingly, the contralateral anterior and posterior legs, i.e. $\mathrm{L_1}$ and $\mathrm{R_3}$, $\mathrm{L_3}$ and $\mathrm{R_1}$, move together in phase. The two limbs of each segment are still half a period (180°) out of phase and the consecutive movements of the limbs are one quarter of a period (90°) out of phase.

Caterpillar is another medium speed gait at which the motion of the left and right limbs are in synchrony (Fig. 1D) according to the scheme:

$$(\mathrm{L_3R_3}),\ (\mathrm{L_2R_2}),\ (\mathrm{L_1R_1}).$$

When an insect moves rapidly, it typically adopts the alternating tripod gait (Fig. 1E):

$$(\mathrm{L_3L_1R_2}),\ (\mathrm{L_2R_3R_1}).$$

In the tripod gait, the ipsilateral anterior and posterior legs, and the contralateral middle leg move together in phase. The limbs of each segment are half a period (180°) out of phase and the adjacent limb on the right and left sides are also half a period (180°) out of phase.

III. Oscillatory modes in the Toda-Rayleigh six-units ring

A. Toda-Rayleigh Ring

Toda [13] provided an exact solutions for a Hamiltonian lattice system with exponential interaction. Figure 2A shows the ring geometry we use. Six (by the number of legs) units are coupled by special springs. The strength of interaction among the nearest units exponentially increases with the decrease of the inter-particle distance (Fig. 2B). Under appropriate limits the Toda interaction goes into the harmonic oscillator or into the hard sphere interaction.

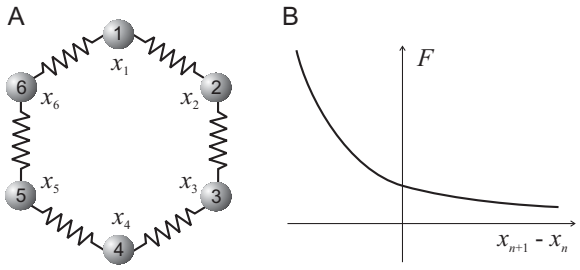

Fig. 2. The Toda ring. A) Six units (particles) are coupled in a ring by "exponential" springs. B) Exponential coupling force acting between pairs of neighboring units.

The Toda system is hamiltonian, whereas its circuit implementation unavoidably has energy loss. Thus any excitation of the circuit decays in time and finally vanish. Accordingly to sustain oscillations we need to supply energy to the system. The energy-dissipation balance can be obtained by the Rayleigh mechanism [12] that includes a cubic nonlinearity in the original Toda system regulating the pumping-dissipation balance [16].

The Toda-Raleigh model [16] in its canonical form is given by:

$$\ddot{x}_n + \omega_0^2(e^{x_n - x_{n+1}} - e^{x_{n-1} - x_n}) - \gamma(\mu - \dot{x}_n^2)\dot{x}_n = 0, \quad (1)$$

where ω_0 is the frequency of linear oscillations, μ is the Rayleigh parameter, and γ defines the weight of the Rayleigh cubic nonlinearity in the dynamics of the ring. In the limit $\gamma = 0$ we have the original Toda equation whose exact solution is a cnoidal wave:

$$e^{x_{n-1}-x_n} = 1 + \left[\frac{2K\nu}{\omega_0}\right]^2 \left(dn^2\left[2K\left(\frac{n}{\lambda} \pm \nu t\right)\right] - \frac{E}{K}\right), \quad (2)$$

where K and E denote the complete elliptic integrals of the first and second kind, respectively, and dn is the Jacobian elliptic function of modulus k. Thus the Toda ring has a continuum of solutions selected by initial conditions.

For $\gamma > 0$ the energy balance admits only a discrete set of solutions. In the truly damped case ($\mu < 0$) the system has only one motionless globally stable solution $\{x_{n+1} - x_n = 1\}$. At $\mu = 0$ the system undergoes a symmetric Hopf bifurcation [16]. The $2N$ (twelve for the six-units ring) eigenvalues of the linearized problem are given by [19]:

$$\delta_m^{1,2} = \frac{1}{2}\left(\gamma\mu \pm \sqrt{\gamma^2\mu^2 - 16\sin^2\left[\pi m/N\right]}\right), \quad (3)$$

where $m = 0, \pm 1, ..., \pm N/2$. One eigenvalue, for $m = 0$, vanishes due to the translation symmetry of the system. Another is real, $\delta_0^2 = \gamma\mu$, and changes sign at $\mu = 0$. The other $2(N-1)$ eigenvalues are complex conjugate and cross, simultaneously, the imaginary axis at $\mu = 0$, obeying Hopf theorem [20].

For positive μ, $(N-1)$ different oscillatory modes appear in the system. These modes correspond to stable limit cycles coexisting in the $2N$ dimensional phase space of the system. They represent nonlinear waves (*acoustic* modes) propagating along the ring and can be labeled by their wave number m. The mode number defines the number of local compressions (wave humps) along the ring. Thus for the six-units ring (Fig. 2A) $m = 1$ corresponds to a single-peak wave; $m = 2$ to a two-peaks wave and $m = 3$ is the so called *optical* mode when the nearest neighbors move in antiphase. The sign in the mode number defines the direction (clockwise or counterclockwise) of the wave propagation. Two other modes, for $m = \pm 0$, correspond to the clockwise and counterclockwise rotations of the ring as a whole. Note that since each mode corresponds to a stable limit cycle, only one mode can be realized in the ring at a time with no superposition admitted. As we shall see further the modes $m = 1$, 2, and 3 correspond to three different gaits of a hexapodal robot.

B. Analog Circuit Implementation

Figure 3A shows a circuit block-scheme for the Toda-Rayleigh ring consisting of six units. Detailed description of all components can be found in [16]. Relative to the circuit previously used here we introduce additional resistors R_B to get the voltage $\widehat{V}$ averaged over all units in the ring. Furthermore, we introduce an amplifier to have the possibility to increase or decrease the voltage $V_{\rm sh}$ applied to the voltage adders. By means of the switch S the input of the amplifier can be connected either to variable voltage source $V_{\rm ext}$ or to the common point providing voltages $\widehat{V}$ (Fig. 3A). In the first case

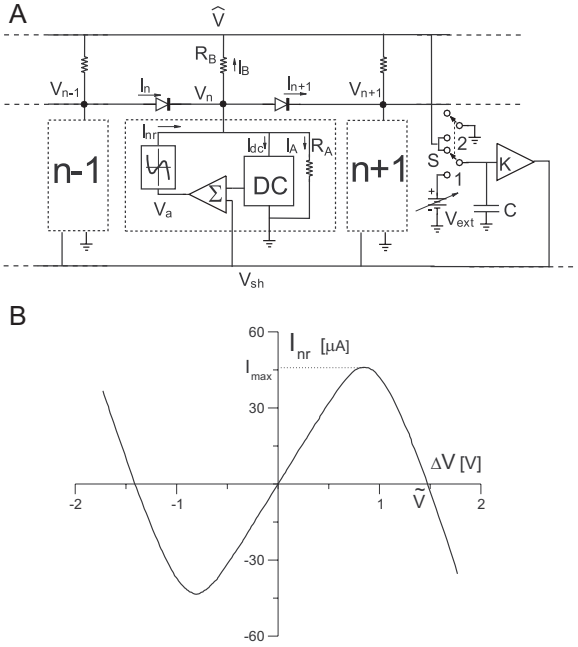

Fig. 3. A) Block scheme of the Toda-Rayleigh ring. Each unit (marked by a dashed box) includes three main blocks: a double capacitor (DC), a nonlinear resistor, and voltage adder providing additional shift of the voltage at the nonlinear resistor accordingly to the common voltage $V_{\rm sh}$. R_A is a stabilizing high value resistor. Resistors R_B are used to obtain voltage $\widehat{V}$ (loosely speaking averaged over the units). The additional circuit (on the right side) including switch S, high capacitance C, external battery $V_{\rm ext}$ and amplifier with variable coefficient k is used to automatically control the dynamics of the ring via the global feedback. B) Experimental current-voltage relation for the nonlinear resistor, $I_{\rm nr}(\Delta V)$, where $\Delta V = V_n - V_b - V_{\rm ext}$ is the voltage applied to its terminals.

resistors R_B are connected in parallel to R_A, hence forming effective resistors of higher conductance. In the second case besides the nearest neighbor coupling via diodes we have a kind of global coupling provided by resistors R_B with a feedback loop via the amplifier to the voltage adders, and finally to the nonlinear resistors. Due to the hight value of R_B this global coupling does not affect directly the dynamics of the circuit, but instead it controls behavior of the ring via the feedback.

According to the current-voltage (I–V) relation of the double capacitor (DC) [21] and to Kirchhoff's laws, we get equations governing the dynamics of the circuit [16], [22]:

$$\frac{d^2V_n}{dt^2} = \omega_v^2 R_{\rm dc}\left(I_n - I_{n+1} + I_{\rm nr} - I_A - I_B\right), \quad (4)$$

where ω_v is a constant depending on the inner components of the double capacitor. $I_{\rm nr}$, I_A and I_B are currents through the nonlinear and two linear resistors in the unit n, respectively (Fig. 3A). I_n represents the current through the junction diode, that can be accurately modeled with

$$I_n = I_s \exp\left(\frac{V_{n-1} - V_n}{V_t}\right), \quad (5)$$

where the constants I_s and V_t depend on the inner diode structure. Thus using diodes we obtain the Toda exponential coupling (Fig. 2B) between neighboring units. Depending on

the position of the switch S, the voltage $\widehat{V}$ can be equal to zero (common point is connected to the ground) or it may vary. The current through the non-linear resistor (block NR in Fig. 3A) $I_{\rm nr}$ is a nonlinear function of the voltage applied to its terminals $\Delta V = V_n - V_a$. The function $I_{\rm nr}$ (Fig. 3B) is a cubic-like with three zeros and positive slope at the origin, hence having a part with negative differential resistance. Accordingly, we have the Rayleigh energy pumping mechanism. Note that the voltage applied to the nonlinear resistor is a linear combination of time derivative of the voltage at the unit, V_n, and the "shift" voltage $V_{\rm sh}$.

IV. Central Pattern Generators Based on the Toda-Rayleigh Electrical Circuit

Let us now show how the symmetries of different gaits shown in Fig. 1 can be modeled by oscillatory modes generated by Toda-Rayleigh electronic circuits.

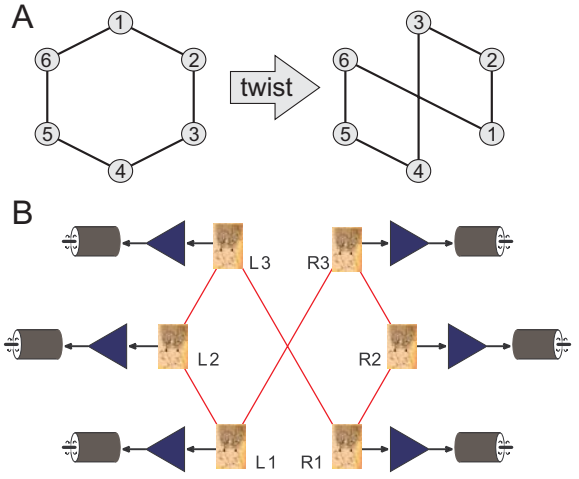

Fig. 4. Hexapod CPG based on the Toda-Rayleigh six-units ring. A) Twisted ring topology. B) Connection scheme of the Toda-Rayleigh units to the limb actuators. Each rectangular block represents a complete electrical unit shown in Fig. 3 coupled through an adapter to the motor driving the corresponding leg.

To accommodate oscillatory modes above described to the gate symmetries we change the initial ring geometry. Figure 4A illustrates how a new twisted topology can be obtained. For the new topology in the clockwise numbering we have the following sequence of units:

$$3 \to 2 \to 1 \to 4 \to 5 \to 6.$$

Note that this sequence is used only for mapping of the oscillators to the limbs, whereas the actual Toda-Rayleigh circuitry remains unchanged. However, this trick helps us to get a direct mapping of the wave modes observed in the electrical circuit to gait symmetries described above (Fig. 1).

We associate each limb with a single oscillator whose dynamics drives through an adapter the corresponding actuator (Fig. 4B). The actuator motor rotates according to the voltage dynamics of the corresponding Toda-Rayleigh oscillator. When the voltage derivative is positive we have the swing phase, whereas the negative derivative corresponds to the stance phase. Then the interlimb coordination will naturally follow from the coupling and dynamical interaction of the oscillators.

Figure 5 show experimental traces of the three oscillatory modes ($m = 1$, 2, and 3) generated by the Toda-Rayleigh six-units ring. The three modes lead to the limb movements with symmetries shown in the lower insets of Fig. 5. Comparing the gaits obtained with the Toda-Rayleigh CPG to the insect gaits shown in Fig. 1 we indeed see that the metachronal, canterpillar and tripod gaits are successfully generated by the CPG (Figs. 5A, 5B and 5C). Note that some overlapping in swing phases observed in Fig. 5 is also observed in the insect gaits.

V. CPG Integrating the Actuator Dynamics in the Gait Control

Denomination as e.g. metachronal gait may lead to a misinterpretation of the gait as being fixed. However, insects (and other animals e.g. crustaceans) make use of free gaits, i.e. the gait characteristics are always changing according to the environment. For example when small obstacle is on the path the swing phase of a leg can be shifted or made shorter.

The earlier CPGs (see e.g. [4], [6]-[11], [18]) and that shown in Fig. 4B always produce the same rhythms (fixed gaits) thus having no account for the dynamics of the robot legs, neither the body. In this section we propose a new circuit implementation for the Toda-Rayleigh ring that includes the robot current state as a variable. Thus the new CPG will be able to change some characteristics of the gait "on the fly".

The idea is to replace the double capacitor (Fig. 3A) by a loop going through the corresponding motor controlling the leg. Figure 6 illustrates how the DC-block can be replaced by the motor-leg-sensor block. Note that the sensor is used only to get the current angle of the motor. As we show below such replacement conserves the main circuit equations describing the dynamics of the Toda-Rayleigh ring. However, through the loop involving the motor we get new parameters directly depending on the leg dynamics. In normal conditions (say when walking over a flat surface), these parameters will be constant not affecting the circuit operation, however, if the environment changes, for instance the robot goes from the horizontal to inclined surface, we get an autonomous tuning of the gait frequency or even a switch to another more appropriated gait for the new scenario.

First we note that, in a quite general case, the dynamics of the motor moving a leg obeys the following equation

$$J\frac{d^2\theta_n}{dt^2} + \nu\frac{d\theta_n}{dt} + \sigma = \Phi I \qquad (6)$$

where θ_n is the angle of the n-th rotor, I is the current thought the motor, J is the momentum of inertia, ν is the friction coefficient, σ is the load torque, and $I\Phi$ is the electromagnetic torque. Note that motor parameters are coupled to the leg dynamics and play a role of the feedback coming from the environment.

Second, by using an angle-voltage converter coupled to the rotor of the motor, we obtain the voltage $V_n(t) = \theta_n(t)/C_v$.

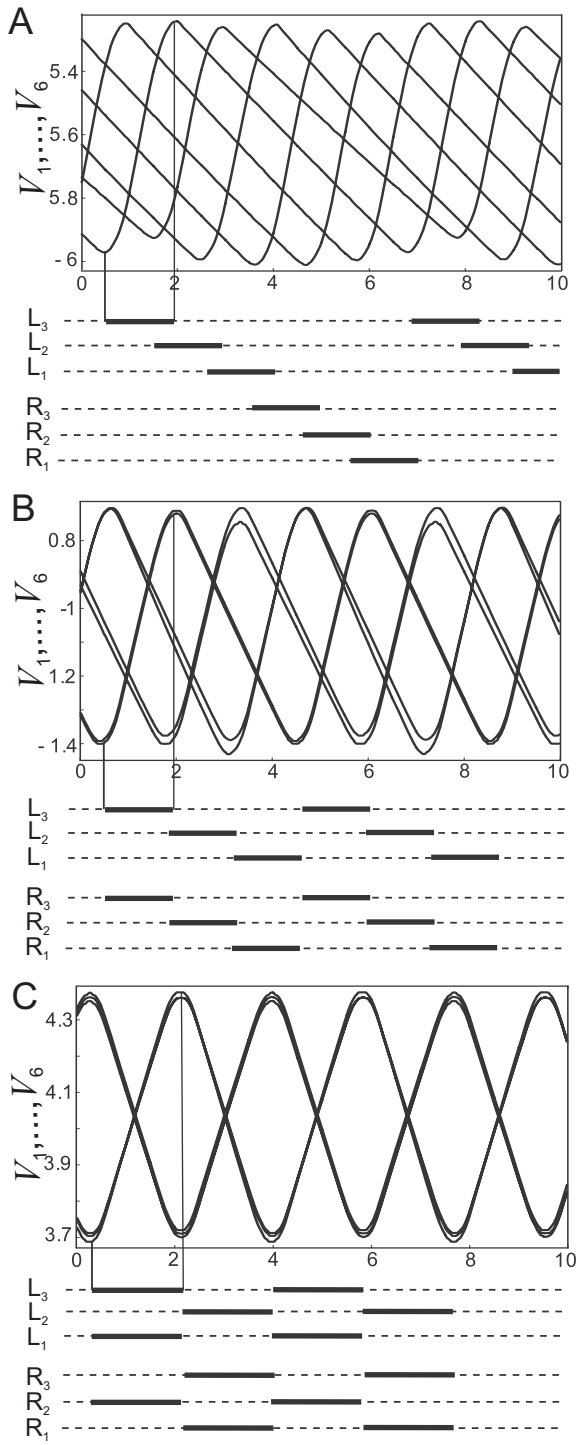

Fig. 5. Oscillatory modes generated by the six-units Toda-Rayleigh circuit and their relations to hexapode gaits. Upper insets show oscilloscope traces of the voltages from all units. Bottom insets show the corresponding phase relations. A) The wave mode with $m = 1$ corresponds to the metachronal gait (compare to Fig. 1). B) The mode $m = 2$ corresponds to the canterpillar gait. C) The optical mode ($m = 3$) models the tripod gait.

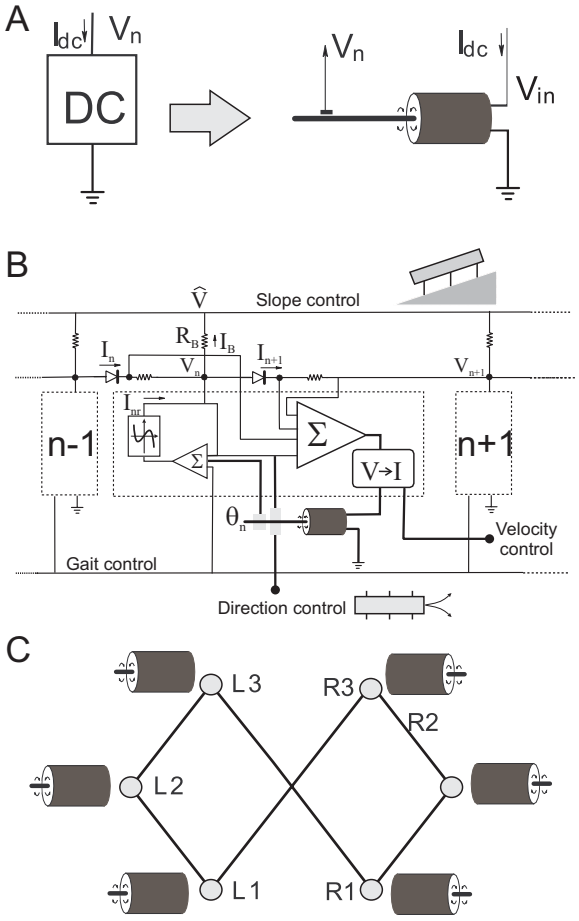

Fig. 6. CPG with the dynamics of the limb actuators integrated into the gate control. A) Scheme showing the point of the circuit to get the values of the variables V_n and I_{dc} in the case of DC block and motor. B) Feedback loop through the robot environment allowing to tune the CPG according to the robot task. DC-block (Fig. 3) is substituted by the motor-leg-sensor block, voltage adder, and voltage to current converter. C) Ring configuration. Filled circles correspond to electrical circuits with the motor dynamics replacing the double capacitors in the circuit.

Then the new variable $V_n(t)$ evolves according to:

$$\frac{d^2V_n}{dt^2} + \nu' \frac{dV_n}{dt} + \sigma' = \alpha I, \tag{7}$$

where α, σ' and ν' are suitable constants.

Third, we can compensate the constant term and first derivative by splitting the current $I = I_v + I_0 + I_{dc}$ (Fig. 6B) obtaining:

$$I_0 = \frac{\sigma'}{\alpha}, \quad I_v = \frac{\nu'}{\alpha}\frac{dV_n}{dt}. \tag{8}$$

Then from Eq. (7) follows:

$$\frac{d^2V_n}{dt^2} = \alpha I_{dc}\,, \tag{9}$$

which is equivalent to the voltage equation of the double capacitor [16], [21]. Thus we obtain Eq. (4) describing the network where instead of the electrical circuit with the double

capacitor we make use of the dynamics of the motors. Accordingly we obtain a feedback coming from the body-leg-motor system.

Note that in the new electrical circuit we use a voltage-current converter (labeled by $V \rightarrow I$ in Fig. 6B) to compensate the difference between Eqs. (4) and (9). Although both expressions are mathematically equivalents, in the case of the DC block, both V_n and I_{dc} correspond to the same conductor in the circuit, whereas in the case of the motor dynamics, those magnitudes refer to different points as it is illustrated in Fig. 6A.

Finally, Fig. 6C shows topology of the new CPG containing six units with motors incorporated into the electrical circuit. This CPG conserves all the gaits of its fixed counterpart, but now parameters of Eq. (4) depend directly from the mechanical characteristic of the hexapod.

VI. Conclusions

We have proposed the use of the Toda-Rayleigh ring as a central pattern generator (CPG) for controlling hexapodal robots. We have shown that in order to model the main gaits, one can use a ring composed of six-units coupled though adaptors to the limb actuators (motors).

To illustrate our results we built an electrical circuit of oscillatory elements and have shown that the dynamical behaviour of the circuit reproduces the phase relationships found in gaits of a six-legged animal. Moreover, changing one external parameter (a voltage) one can switch between different modes or gaits.

Then we have proposed a method allowing natural incorporation of the actuator (motor) dynamics in the CPG. With this approach we close the loop CPG – environment – CPG, thus obtaining a decentralized model for the leg control. Such novel model does not require higher level intervention to the CPG for locomotion in a nonhomogeneous environments.

References

[1] E. Kandel, J. Schwartz, and T. Jessell, *Principles of Neural Science*. Kandel and Schwartz Ed., Elsevier 1991.
[2] C. A. Wiersma (ed.) *Invertebrate nervous systems*. Univ. Chicago Press 1968.
[3] H. Cruse, "What mechanisms coordinate leg movement in working arthropods?", *Trends in NeuroScience*, vol. 13, pp. 15–21, 1990.
[4] M. Golubitsky, I. Stewart, P.-L Buono, and J. J. Collins, "Symmetry in locomotor central pattern generators and animal gaits", *Nature*, vol. 401, pp. 693–695, 1999.
[5] H. Cruse, T. Kindermann, M. Schumm, J. Dean, and J. Schmitz, "Walknet - a biologically inspired network to control six-legged walking", *Neural Networks*, vol. 11, pp. 1435, 1998.
[6] P. Arena, L. Fortuna, and M. Branciforte, "Reaction-diffusion CNN Algorithms to Generate Artificial Locomotion", *IEEE Trans. Circuits Systems* I, vol. 46, pp. 253, 1999.
[7] W. Y. Yiang, G. Schooner, and J.A.S. Kelso, "A synergetic theory of quadrupedal gaits and gait transition", *J. Theor. Biol.* vol. 142, pp. 359–391, 1990.
[8] J. J. Collins and I. Stewart, "Coupled nonlinear oscillators and the symmetries of animal gaits" *Nonlinear Science*, vol. 3, pp. 349–392, 1993.
[9] J. J. Collins and I. Stewart, "Hexapodal gaits and coupled nonlinear oscillator models". *Biological Cybernetics* vol. 68, pp. 287–298, 1993.
[10] J. J. Collins and I. Stewart, "A group-theoretic approach to rings of coupled biological oscillators", *Biological Cybernetics* vol. 71, pp. 95–103, 1994.
[11] M. Golubitsky, I. Stewart, P. L. Buono, and J. J. Collins, "A modular network for legged locomotion", *Physica D* vol. 115, pp. 56–72, 1998.
[12] J. W. Rayleigh, *The Theory of Sound* 2nd ed., Dover N.Y., 1945.
[13] M. Toda, *Theory of Nonlinear Lattices*, Springer Berlin, 1981.
[14] M. Toda, *Nonlinear Waves and Solitons*, Kluwer Dordrecht, 1983.
[15] V. A. Makarov, W. Ebeling, and M. G. Velarde, "Soliton-like waves on dissipative Toda lattices", *Int. J. Bifurcation and Chaos* vol. 10, pp. 1075–1089, 2000.
[16] V. A. Makarov, E. Del Rio, W. Ebeling, and M. G. Velarde, "Dissipative Toda-Rayleigh lattice and its oscillatory modes", *Physical Review E* vol. 64, pp. 036601–36615, 2001.
[17] E. Del Rio, V. A. Makarov, M. G. Velarde, and W. Ebeling, "Mode transitions and wave propagation in a driven-dissipative Toda-Rayleigh ring", *Physical Review E* vol. 67, pp. 056208–056217, 2003.
[18] S. Still, K. Hepp, and R. J. Douglas, "Neuromorphic walking gait control", *IEEE Trans. Neural Netw.* vol 17, pp. 496–508, 2006.
[19] V. A. Makarov, M. G. Velarde, A. Chetverikov, and W. Ebeling, "Anharmonicity and its significance to non-Ohmic electric conduction", *Physical Review E*, vol. 73, pp. 066626-066612, 2006.
[20] Yu. A. Kuznetsov, *Elements of Applied Bifurcation Theory*, Springer-Verlag, Berlin, 1995.
[21] A. C. Singer and A. V. Oppenheim, "Circuit implementation of soliton systems", *Int. J. Bifurcation Chaos* vol. 9, pp. 571, 1999.
[22] N. Islam, J. P. Singh, and K. Steiglitz, "Soliton phase shifts in a dissipative lattice", *J. Appl. Phys.* vol. 62, pp. 689–693, 1987.